Experimental analysis of sound directivity from sound propagation through non-isothermal, turbulent exhaust jets in cross-flow

Orddom Yi Jie Leav (1), Benjamin Seth Cazzolato (1) and Carl Quentin Howard (1)

(1) School of Mechanical Engineering, University of Adelaide, Adelaide, Australia

ABSTRACT

The common assumption when predicting community noise levels from exhaust stacks is that the sound radiation is axisymmetric, which is appropriate for low Mach number, low temperature flows, and in the absence of cross-winds. However, this assumption is inaccurate when the conditions do not hold. This paper investigates experimentally the effects of a cooler cross-flow on the sound directivity of turbulent, heated exhaust gas from a stack. A small-scale experimental rig (1:100) has been built that reproduces the flow, temperature and acoustic conditions seen in large-scale open-cycle gas turbines. The University of Adelaide's Wind Tunnel was used to create cross-flows that resemble the cross-wind conditions observed near open-cycle gas turbines. The small-scale experimental rig and the test conditions were scaled using relevant non-dimensional fluid dynamics and acoustic parameters. Directivity measurements from the experiments have shown that the hot exhaust plume leads to an asymmetric acoustic radiation pattern from the exhaust stack. The experimental results presented in this paper shows that the presence of a hot exhaust plume and cross-flow alters sound directivity in the far-field downstream by increasing levels up to 11 dB, which has the potential to impact nearby communities.

1 INTRODUCTION

Sound propagation models for environmental noise prediction commonly assume that sound radiates as an elevated monopole source. However, when there are complex flow conditions affecting refraction, structures scattering and diffracting sound and meteorological effects, this assumption may not be appropriate. An example of such a case is modelling sound radiation from open-cycle gas turbines (OCGT), which has been shown in literature to produce higher than expected low frequency noise levels in communities (Bjork 1994, Broner 2010, 2011, 2012, Hessler Jr 2004, 2005, Hetzel and Putnam 2009, Kudernatsch 2000). It has been reported that the low frequency noise levels from OCGT have caused the following impact on communities: perceived 'annoyance' of throbbing (Broner 1978), 'beating' sensation in the chest (Hessler Jr 2004, 2005), nausea (Broner 1978), and acoustic excitation in structures with low resonance frequencies (Broner 1978). The higher than expected noise levels observed in OCGT are not typically seen in combined cycle gas turbines, which use the Brayton and Rankin cycle (Bjork 1994, Hetzel and Putnam 2009).

Sound levels in neighbourhoods near exhaust stacks are commonly predicted using multiple ISO standards (International Organization for Standardization 1993a, b, 1996). ISO 10494 is used to estimate the sound power from exhaust stacks (International Organization for Standardization 1993b). The sound propagation is modelled using ISO 9613-1 (International Organization for Standardization 1993a) and ISO 9613-2 (International Organization for Standardization 1996). For simple sound predictions ISO 9613-2 states that a simple monopole source can be used, but for more complex sound sources, a directivity correction factor can be applied. If a single monopole source cannot be used, then multiple monopole sources can be used to represent a discretised line source or discretised area sound source. A single value correction factor based on the meteorological conditions obtained from the 'local authorities' can be applied to the sound propagation model. These sound prediction models can also be extended using numerical software to include the atmospheric boundary layer (thermal and velocity gradients) and complex terrains. These approximations do not take into consideration the complex sound field from the exhaust stack and the acoustic interaction with the exhaust plume.

The fluid dynamics associated with non-isothermal exhaust stacks can be simplified to an elevated jet in cross-flow (JICF), which can be seen schematically in Figure 1 (Adaramola, Sumner, and Bergstrom 2010). The elevated JICF is a cylindrical duct protruding from a ground plane, with a jet flow exiting the duct. The flow structures associated with isothermal elevated JICF have been studied experimentally by various researchers in the literature (Adaramola, Sumner, and Bergstrom 2010, Eiff, Kawall, and Keffer 1995, Eiff and Keffer 1997, Hsu and

Huang 2012, 2014, Huang, Davidson, and Nokes 2005, Huang and Hsieh 2002, 2003, Huang and Hsu 2012, Huang and Lan 2005) and non-isothermal elevated JICF have also been investigated (Andreopoulos 1989a, b, Johnson, Elliott, and Christensen 2013). The fluid structures are governed by the JICF momentum flux ratio, defined as the following:

$$R = \sqrt{\frac{\rho_j u_j^2}{\rho_{cf} u_{cf}^2}}, \tag{1}$$

where ρ_j is the jet air density, ρ_{cf} is the cross-flow free stream air density, u_j is the average jet exit velocity, and u_{cf} is the cross-flow free stream velocity. The values for *R* in OCGT are typically in a 'jet-dominated' regime (Adaramola, Sumner, and Bergstrom 2010, Huang and Hsieh 2002, 2003, Johnson, Elliott, and Christensen 2013), in which the flow structures associated with this regime are shown in Figure 1. The unique flow structures that form for this regime are the following: deflected jet, jet shear layer, counter rotating vortex pairs, and stack shear layer (Adaramola, Sumner, and Bergstrom 2010).

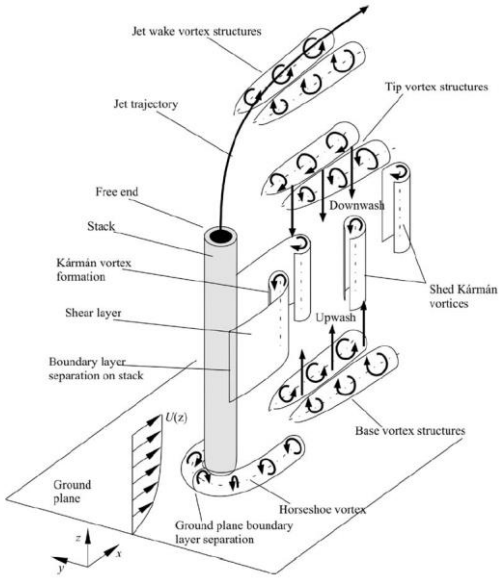

Source (Adaramola, Sumner, and Bergstrom 2010)

Figure 1: Flow structures schematic for elevated jets in cross-flow in the jet dominated regime

Research has shown that the radiation propagation from exhaust ducts may be quite complex. Bies, Hansen, and Howard (2017) showed that the sound radiation from exhaust ducts in the absence of flow in an anechoic environment is highly directed, with a lobe forming on-axis as the acoustic frequency increases. For non-isothermal exhaust duct flows a jet shear layer forms. It is known that with the presence of a shear layer sound refraction occurs (Amiet 1978, Candel 1972). The sound refraction due to the shear layer can be extended to non-isothermal jet shear layers, showing significant sound refraction (Atvars et al. 1965, Atvars, Schubert, and Ribner 1965, Grande 1965). The change in sound directivity from sound refraction becomes more pronounced with an increase in jet Mach number M_j, jet temperature T_j, and acoustic frequency. Mungur, Plumblee, and Doak (1974) showed that for isothermal jets, the location at which the sound directivity measurements are taken is also critical, with the developing jet shear layer downstream causing continual refraction many diameters from the exhaust outlet. This work on jet shear layer refraction was also extended to OCGT exhaust flow with near-field measurements by Bjork (1994). The research has shown that the sound is refracted by the jet shear layer and this was measured in both a real OCGT exhaust stack and in a scaled model (Bjork 1994).

It is hypothesised that sound radiating from OCGT exhaust stacks forms strong lobes, that under certain meteorological conditions, leads to the amplification of sound downstream as it interacts with the bent-over hot exhaust plume. Earlier work by Bjork (1994), stated that a bent-over hot exhaust plume with the thermal gradients and varying wind conditions would cause variations in sound levels downstream of up to $\pm$5 dB in the neighbourhood. However, Bjork (1994) only measured the sound in the near field; from the real exhaust stack at approximately 1.5*D* and approximately 3*D* with the small scale model, where *D* is the internal duct diameter. In the near-field the onset of refraction begins and cross-flow effects are yet to occur. Work previously done by (Leav, Cazzolato, and Howard) (2015, 2017) has shown numerically that the propagation path of sound is affected by the temperature of the plume for 2D non-isothermal ground level JICF and for 3D elevated JICF. Leav, Cazzolato and Howard (2015, 2017) have shown the propagation path of sound is dependent on the acoustic frequency and the distance from the exhaust outlet. Upstream of the exhaust stack the sound remains relatively unaffected by the cross-wind, with elliptical acoustic spreading observed (Leav, Cazzolato, and Howard 2017). Downstream of the exhaust stack for both the 2D non-isothermal ground level JICF and the 3D elevated JICF, the sound is altered and forms a highly directed lobe of sound. The numerical simulations were conducted using steady-state simulations with isotropic Reynolds-averaged Navier-Stokes equations (RANS) models which leads to limitations. The highly unsteady transient small-scale structures are not reproduced using RANS in Computational Fluid Dynamics (CFD). Furthermore, the steady state CFD model also produces coherent vortex structures downstream (counter rotating vortex pairs) that in reality would dissipate with the presence of the turbulence structures from the incoming cross-flow. The counter rotating vortex pairs downstream provide a thermal gradient that enables continuing refraction as the sound propagates downstream. For the 3-D elevated JICF, the acoustically reflective duct and ground produces complex sound diffraction patterns (Leav, Cazzolato, and Howard 2017).

This paper experimentally investigates the sound directivity of a non-isothermal, elevated hot exhaust jet in cooler cross-flow. A reduced scale (1:100) experimental rig to reproduce the flow and acoustic conditions of a 150 MW OCGT has been designed and commissioned at the University of Adelaide's Wind Tunnel. The experimental findings from the reduced scale experiments are used to analyse the effects of the plume on the propagation of sound. The layout of the paper is as follows. A description of the experimental set up and the signal processing techniques used for acoustic measurements are discussed in Section 2. In Section 3 the acoustic directivity measurements are detailed. A discussion of the experimental findings in relation to real OCGT is presented in Section 4. The main conclusions of the paper are summarised in Section 5.

2 APPARATUS AND METHODOLOGY

Measurements of OCGT are complex due to the practicality of controlling flow and speed, as well as taking measurements to characterise flow temperature, flow speed, and sound pressure. The aim of this research is to simulate the flow, temperature and acoustic parameters of a full-scale OCGT with a small-scale exhaust rig where the relevant parameters can be controlled. This section will discuss the experimental apparatus representing the OCGT, the commissioning of the experimental apparatus at the University of Adelaide Wind Tunnel, instrumentation, and the signal processing techniques used to process the acoustic data.

The experimental apparatus for simulating the exhaust flow and sound is shown in Figure 2. The exhaust was designed to achieve the parameters in Table 1. It should be noted that the exhaust rig was designed based on non-dimensional acoustic parameters relevant to OCGTs, but where possible the non-dimensional fluid dynamic parameters were also considered. An AIRPACK centrifugal blower was used to create the flow in the duct network. The inlet and outlet of the blower were connected to a silencer on each end. The flow travelled through a stainless-steel duct network with an outer diameter of 50.8 mm and an inner diameter of 47.6 mm (*D*), which is designed to be approximately 1:100 scale of a real 150 MW OCGT. The flow from the outlet silencer to the AIRPACK blower was split into a Y-junction and was passed through two 16kW LEISTER 61L System air heaters capable of variable temperature control, and then joined again with a 45° Y-junction into a single flow. The flow in the duct network was measured with a Pitot tube and a differential pressure transducer. The temperature in the duct network was measured with k-type thermocouples. The flow then passed through a 90° bend to a catalytic converter that acted to straighten the flow. The flow then passed through a straight vertical section of pipe before it exited as a jet. The exhaust network was clad with Rockwool SPI insulation to reduce the heat loss in the pipe network and attenuate structural acoustic radiation.

a)

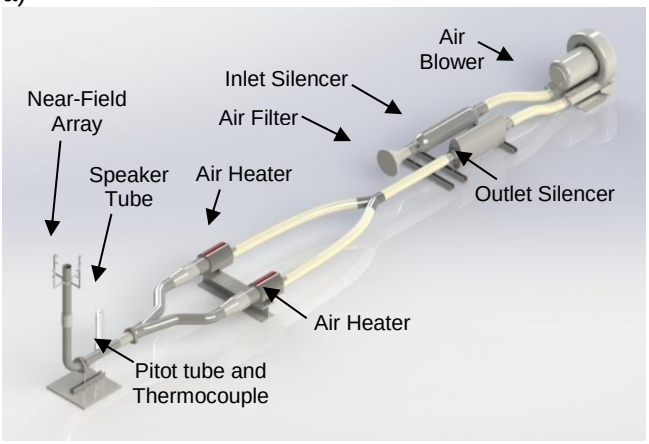

b)

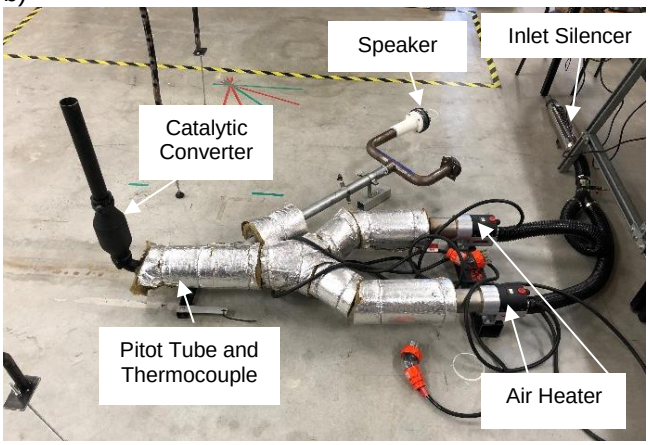

Figure 2: Images of the experimental setup of the reduced scale exhaust network, where a) is a computer aided design model of the exhaust, and b) is a photo of the exhaust network before installation of the false floor (blower not connected).

Table 1: Physical parameters for the experimental tests.

Parameters	Equation/Expression	Value
Mach number	$M = \frac{u_j}{c_j}$	0.1
Helmholtz number	$ka = \frac{\pi f D}{c_j}$	1.1
Jet temperature	T_j	500 °C
Exhaust vertical duct length	$L = 10D$	476 mm
Jet to cross-flow momentum flux ratio	$R = \sqrt{\frac{\rho_j u_j^2}{\rho_{cf} u_{cf}^2}}$	5

Figure 3 shows the experimental setup in the University of Adelaide's Wind Tunnel. A wooden decking, acting as a ground plane, was placed over the exhaust rig. Acoustic foam (50 mm thick Dacron) was placed on the wooden decking to reduce acoustic reflections from the ground plant and to provide an anechoic surface above 500 Hz, thereby reducing the complexity of the sound field so that the effect of the plume, cross-flow and sound interaction can be examined. The wooden decking is used so that only the exhaust stack interacts with the flow, with the rest of the apparatus shielded from the flow. The cross-sectional area of the wind tunnel cross-flow is 2.75 m × 2 m and the available test section ground area covers a span of 3.5 m × 5.5 m. The cross-flow wind velocity was measured with a Cobra Probe 209 and a Fluke 922 airflow meter at discrete points in the cross-flow freestream velocity.

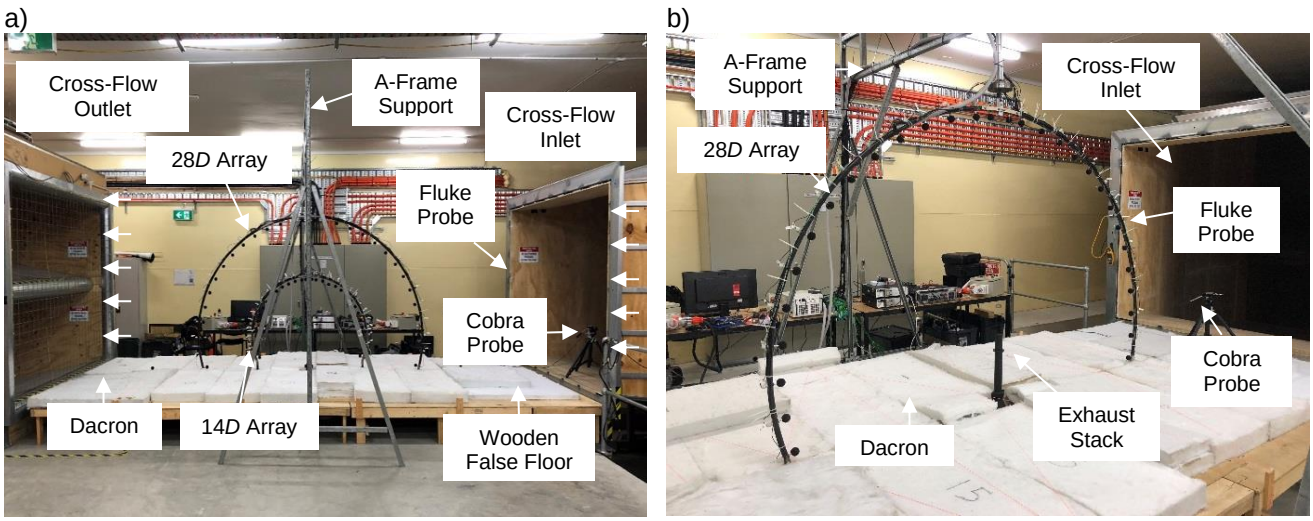

Figure 3: Photo of the experimental setup at the University of Adelaide's Wind Tunnel with the cross-flow going from right to left in all figures, where a) photo showing the full span of the commissioned test set up, b) the experimental set up with only the 28*D* microphone array.

The sound pressure was measured with 62 G.R.A.S. 40PH Free-Field Microphones along two circular arrays with radii 14*D* and 28*D* from the exhaust stack outlet. The microphones in Figure 3 were placed along a circular arc spanning $\pm$ 105°, with each microphone spaced 7.5°, except for the centre microphone at 0° being replaced by two microphones at $\pm$ 2.5° for the 14*D* array arc and for the 28*D* arc the centre microphone at 0° was removed to accommodate the vertical support. The microphone arrays were positioned parallel to the cross-flow free stream. The microphone arrays were supported by a frame, designed to have minimal flow and acoustic impact. The microphone signals were recorded by a NI (National Instruments) PXIe-4499 Sound and Vibration Module in a NI PXIe 1082 Chassis. The sound source used was uniform white noise, generated from NI LABVIEW and the electrical signal was generated using a NI PXI-6221 Multifunction I/O Module. The sampling frequency was 25.6 kHz. The uniform white noise was passed through a dual channel analogue 4-pole Butterworth filter (Krohn-Hite Model 3362 Dual Channel Filter) designed with low-pass and high-pass filter to give a 4kHz one-third octave ($ka \approx 1.1$). The sound was generated using two compression drivers, a 50.8 mm (2 inch) DS18 PRO-DKH1 1000 W compression driver and the 50.8 mm (2 inch) TIMPANO TPT-DH2000 400 W compression driver.

The acoustic data was post-processed in the frequency domain using MATLAB. The spectral analysis used a Hanning window with an FFT length of 8092 and 375 averages. The degree of linearity between the acoustic-electrical signal generated by the DAQ (x) and the acoustic pressures measured at the microphones (y) may be quantified using the coherence function:

$$\gamma_{xy}^2(f) = \frac{|G_{xy}(f)|^2}{G_{xx}(f)G_{yy}(f)}, \tag{1}$$

where f is the frequency of interest, G_{xy} is the cross power spectra of the acoustic-electrical signal into the speaker and the microphone acoustic pressures, G_{xx} is the power spectra of the acoustic-electrical signal into speaker and G_{yy} are the power spectra of the microphone acoustic pressures. The results in this paper are presented as the coherent output power at each microphone given by the following formula:

$$COP(f) = G_{yy}(f) \times \gamma_{xy}^2(f). \tag{2}$$

The coherent output power was used, rather than the sound pressure levels, so that only sound correlated with the loudspeaker is analysed, and noise from the blowers, wind tunnel fan and flow induced noise is ignored. The acoustic results for directivity presented in Section 3 are calculated as:

$$DI(f,\theta) = \frac{COP(f,\theta)}{COP_{av}}, \quad (3)$$

where DI is the directivity index based on the coherent output power and not the standard formulation involving sound intensity (Bies, Hansen, and Howard 2017), θ is the angular position from the centreline of the duct, and COP_{av} is the average coherent output power along the directivity arc. This method of presenting the coherent results was chosen to ensure that the sound presented was coherent with the loudspeaker only and the incoherent sound from external sources are 'screened out' and not considered.

3 EXPERIMENTAL RESULTS

The results for the sound directivity in the absence of the heated jet and cross-flow are discussed first. The results for the sound directivity for a heated jet with and without cross-flow are then presented for the 4 kHz one-third octave band.

Figure 4a shows the experimental results for the sound directivity at a distance of 28*D* in the absence of the heated jet and cross-flow. As expected for the 4 kHz one-third octave band ($ka \approx 1.1$), the sound directivity is axisymmetric and elliptical, with a lobe forming along the centreline of the duct axis at 0°. The results in Figure 4a show very similar trends to the results in literature for the open radiation of duct directivity in anechoic environments (Bies, Hansen, and Howard 2017). In the absence of the flow, it is commonly assumed that the sound power can be estimated with ISO 10494 (International Organization for Standardization 1993b) in the near field and then propagated using ISO 9613-2 (International Organization for Standardization 1996), where a monopole assumption is used, which approximates the sound radiation of a piston in an infinite plane. This is not the case seen in the experimental results, and it can be observed that with the hard duct exterior and the anechoic ground, the sound radiation is elliptical with a lobe forming on-axis (0 degrees). In Figure 4a, the elliptical lobe also causes a reduction in sound levels of up to 4.5 dB at ±90°. However, for predictions of ground-level SPLs, the monopole assumption is likely to be conservative.

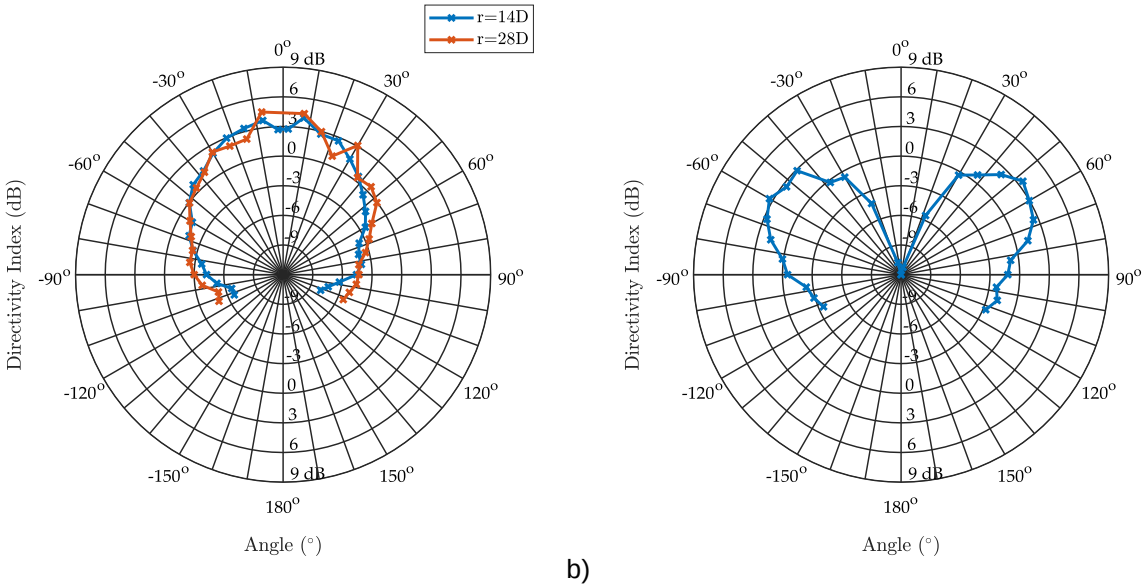

a) b)

Figure 4: The directivity of sound (a) in the absence of flow at two radii (14*D* and 28*D*), and (b) with a jet at 350°C and in the absence of cross-flow at a radius of 28*D*.

Figure 4b shows the experimental results for the sound directivity at 28*D* with a heated jet of Mach number 0.1 and T_j =350 °C. The directivity plot shows that the sound is axisymmetric about the vertical axis, with a shadow zone or 'cusp' forming along the centreline of the duct axis (0°). The acoustic cusp has a Directivity Index of approximately -12 dB. The acoustic energy that was originally in the on-axis region has been refracted by the jet shear layer to form acoustic lobes off-axis at approximately symmetrical locations of ±50°. The SPL of the lobes off-axis have increased by approximately 3 dB, compared with Figure 4a. These results are qualitatively consistent

from the results by Atvars, Schubert, and Ribner (1965) and Bjork (1994). However, it should be noted that the experimental results in this study were measured at a lower jet temperature ($T_j = 350$°C) than commonly seen in OCGT exhaust stacks. The lower temperature used in the tests is a limitation of the experimental setup, where the air temperature at the microphones on the 28*D* arc could exceed the 60°C temperature rating of the microphones. Furthermore, it was desirable to measure the directivity at 14*D* to observe the effects of distance on the sound propagation, in particular the refraction of sound as a result of the jet shear layer, but unfortunately the microphone temperature limits were exceeded necessitating their removal.

Figure 5 shows the experimental result for the sound directivity at 14*D* and 28*D* of a heated JICF with a Mach number of 0.1, $T_j = 500$°C and $R = 5$. Note that the cross-flow permitted higher stack exhaust temperatures whilst remaining under the 60°C temperature limit at the microphone locations. By comparing Figure 4a, Figure 4b, and Figure 5, it can be observed that with the heated plume and cross-flow, the sound directivity is no longer elliptical or axisymmetric about 0°. The directivity of sound becomes biased towards the leeward side (or downstream) of the exhaust duct. The cross-wind shifts the peak observed in the downstream lobe from an angle of 50° to 65° and 90° for the 14*D* and 28*D* array, respectively. It can also be observed that as the sound propagates downstream the width of the lobe decreases from 40° to 25° for the 14*D* and 28*D* arcs, respectively. As the downstream lobe bends over and becomes narrower, the energy becomes more concentrated, increasing in amplitude by 4.5 dB at 14*D* and 6.5 dB at 28*D*. However, upstream of the exhaust duct, the sound directivity patterns remain similar for the 14*D* and 28*D* arcs. The position of the acoustic 'cusp' or shadow zone shifted from 0° in Figure 4b in absence of the cross-flow to 10° at 14*D* and 20° at 28*D* with cross-flow present. It must be noted that the angular resolution of the directivity measurements is 7.5° increments and this may be insufficient in capturing fine detail in the directivity pattern. The directivity results in Figure 5 at the 28*D* array show that the downstream lobe may not be fully resolved for the current angular spacing of the microphones, but for this research it is sufficient in investigating the change in sound levels downstream of the exhaust duct. In summary, the sound directivity is dependent on the arc radii with: the change in the width of the acoustic lobe downstream, the position of the acoustic lobe downstream and the shift in the position of the acoustic 'dip'. As sound propagates downstream, it can be observed that the plume has a greater influence on the propagation path. The influence on the propagation path of sound is strongly governed by the temperature gradients in the plume, which causes the sound to continually refract as it propagates downstream.

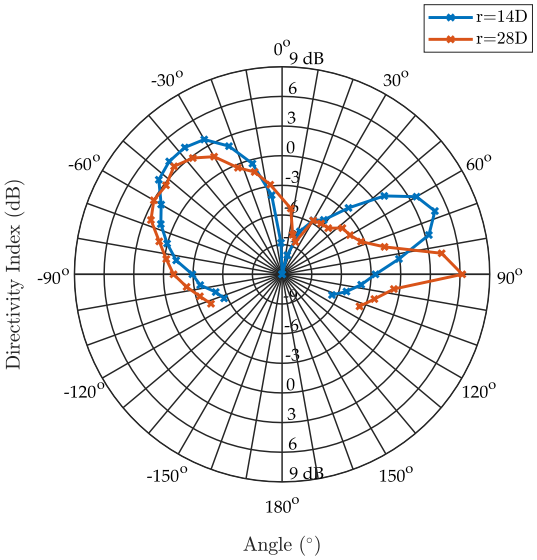

Figure 5: Directivity of sound at two different radii (14*D* and 28*D*), while $R = 5$ and the $T_j = 500$°C. The cross-flow is from left to right.

4 DISCUSSION

The sound propagation downstream of the exhaust duct is altered significantly as it is refracted by the bent-over non-isothermal plume, with refraction being the dominant mechanism for altering sound propagation. The acoustic refraction downstream is due to the temperature and velocity gradients in the plume that alter the speed of sound (*c*) of the air. The majority of the refraction arises from the temperature gradients causing a change in the speed of sound ($\Delta c \propto \sqrt{\Delta T}$), as opposed to the convective effects of the flow ($\Delta c = c + \Delta u_{flow}$). Work previously conducted by Leav, Cazzolato, and Howard (2017) showed that the counter rotating vortex pairs produce thermal and velocity gradients. In their numerical work, the refraction continued for the entire computational domain. Figure 5 shows the relationship with the plume development, and acoustic refraction is consistent with the experimental directivity measurements in this paper at 14*D* and 28*D*. Further experimental investigations will need to examine the directivity at radii greater than 28*D* to quantify far-field magnitude of the directivity index. The flow and temperature field associated with the experimental small-scale model will need to be measured to gain a better understanding on the fluid dynamic and temperature effects that govern the propagation path of sound.

In Figure 5, the experimental results have shown that for $ka \approx 1.1$ (4 kHz one-third octave band) there is a downstream lobe forming causing an increase in sound levels of up to 6.5 dB. The increase in downstream sound level, shown in Figure 5, was calculated using the average coherent output power COP_{av} of that measurement arc. The results can be directly compared to the case without flow, seen in Figure 4a, which results in an elliptical sound radiation pattern. In Figure 4a, the sound downstream at -90° is approximately -4.5 dB, whereas the sound levels in Figure 5 with the bent-over non-isothermal plume is 6.5 dB. Hence, in Figure 5, the plume has caused an 11 dB increase in the sound level parallel to the ground plane when compared to the sound radiation in the absence of flow, as seen in Figure 4a.

The geometry of the reduced scale mode exhaust stack is a simple straight duct section that protrudes 10*D* into the flow. In real OCGTs, the geometry of the plant is considerably more complex, thereby affecting the cross-flow and consequently the sound refraction. This simplification of the model is appropriate for scientific investigation, as it resembles elevated jets in cross-flow seen in literature and reduces the acoustic and fluid dynamic complexity in the model. The main purpose of the research is to investigate the sound interaction with the plume and observe non-axisymmetry of the acoustic directivity, as well as the increase in sound level downstream, which was confirmed in the experimental results here, and previously in numerical studies.

In the experimental worked conducted here, measurements were taken with an anechoic ground to simulate an absorptive surface surrounding the stack. This is generally not the case for OCGTs, as the exhaust stacks are typically surrounded by complex structures and hard reflective surfaces. These reflective surfaces would change the sound directivity pattern and hence the experimental setup used here may not be an accurate representation of real installations. Work completed by Leav, Cazzolato, and Howard (2017) suggests that a complex acoustic pattern occurs when a reflective ground is included. As a result, Figure 4a, Figure 4b and Figure 5 show 'smooth' directivity patterns in the absence of diffraction and reflections from other surfaces. Additionally, the sound directivity results in this paper are presented as a single one-third octave band average to reduce the complexity of the results. Further tests over several one-third octave bands should be undertaken to examine the relationship of the plume and the downstream sound levels.

5 CONCLUSIONS AND FUTURE CONSIDERATION

The results from this experimental study have shown that for $ka \approx 1.1$ (4 kHz one-third octave band) a non-isothermal jet with cooler cross-flow can significantly alter the directivity of sound. In the absence of the jet plume and the cross-flow, the sound is axisymmetric and elliptical with a lobe forming along the vertical axis and reflects current ISO standards. The directivity of sound with the jet shows that the sound is axisymmetric, but strong side lobes form due to sound refraction because of the temperature gradients in the jet shear layer. The presence of a cooler cross-flow causes the sound to be asymmetric, with the sound biased towards the leeward side (downwind) of the exhaust stack. The sound refracts as it travels from the outlet. It was found from these experiments that sound was strongly refracted at a distance of 28*D* downstream from the exhaust duct, resulting in an 11dB increase in sound level, with the beam of sound being closer to the ground level and being more directed or 'narrow', compared to the case in the absence of jet and cross flows.

The current experimental work presented in this paper is a preliminary investigation into the problem and more work is planned to further understand this issue. Firstly, the sound propagation downstream is dependent on the acoustic frequency and other one-third octave bands should be investigated. The microphone arrays can be rotated through the vertical axis and measurements taken to explore the asymmetric spreading. The effects of cross-flow free stream velocity on the sound directivity should be investigated. In Section 3, it was noted that the acoustic results for the presence of the non-isothermal plume could be better resolved by increasing the number of microphones on the 28*D* array and reduce the angular separation between microphones. As discussed in Section 4, an investigation into a larger domain should be conducted to observe the limits of acoustic refraction. The flow and temperature field associated with the elevated JICF should be investigated to gain a better understanding on the mechanisms involved with changing the sound propagation path.

ACKNOWLEDGEMENTS

The author was sponsored by an Australian Government Research Training Program Scholarship from 2015 to 2018.The authors would like to thank Ben Wake, Carl Jungfer, and Lauren Manser for their effort as Engineering Honours Students in 2016 in designing and building the reduced scale experimental apparatus for testing at the Thebarton Wind Tunnel.

REFERENCES

Adaramola, M. S., D. Sumner, and D. J. Bergstrom. 2010. "Effect of velocity ratio on the streamwise vortex structures in the wake of a stack." *Journal of Fluids and Structures* 26 (1):1-18.

Amiet, R. K. 1978. "Refraction of sound by a shear layer." *Journal of Sound and Vibration* 58 (4):467-482.

Andreopoulos, J. 1989a. "Wind tunnel experiments on cooling tower plumes: Part 1 in uniform crossflow." *Journal of Heat Transfer* 111 (4):941-948.

Andreopoulos, J. 1989b. "Wind tunnel experiments on cooling tower plumes: Part 2 in a nonuniform crossflow of boundary layer type." *Journal of Heat Transfer* 111 (4):949-955.

Atvars, J., L. K. Schubert, E. Grande, and H. S. Ribner. 1965. Refraction of sound by jet flow or jet temperature. University of Toronto: Institute for Aerospace Studies.

Atvars, J., L. K. Schubert, and H. S. Ribner. 1965. "Refraction of sound from a point source placed in an air jet." *The Journal of the Acoustical Society of America* 37 (1):168-170.

Bies, D. A., C. H. Hansen, and C. Q. Howard. 2017. *Engineering Noise Control: Theory and Practice*. Edited by C. R. C. Press. 5th ed: CRC Press.

Bjork, E. A. 1994. "Experimental study of measures to reduce noise radiated from power-station exhaust stacks." *Noise Control Engineering Journal* 42 (5):171-178.

Broner, N. 1978. "The effects of low frequency noise on people - A review." *Journal of Sound and Vibration* 58 (4):483-500.

Broner, N. 2010. "A simple criterion for low frequency noise emission assessment." *Journal of Low Frequency Noise, Vibration and Active Control* 29 (1):1-13.

Broner, N. 2011. "A simple outdoor criterion for assessment of low frequency noise emission." *Acoustics Australia* 39 (1):7-14.

Broner, N. 2012. "Power to the People." 15th International Meeting on Low Frequency Noise and Vibration and its Control Stratford upon Avon, United Kingdom, 22-24 May.

Candel, S. M. 1972. "Acoustic transmission and reflection by a shear discontinuity separating hot and cold regions." *Journal of Sound and Vibration* 24 (1):87-91.

Eiff, O. S., J. G. Kawall, and J. F. Keffer. 1995. "Lock-in of vortices in the wake of an elevated round turbulent jet in a crossflow." *Experiments in Fluids* 19 (3):203-213.

Eiff, O. S., and J. F. Keffer. 1997. "On the structures in the near-wake region of an elevated turbulent jet in a crossflow." *Journal of Fluid Mechanics* 333:161-195.

Grande, E. 1965. "Refraction of injected sound by a very cold nitrogen jet." *The Journal of the Acoustical Society of America* 38 (6):1063-1064.

Hessler Jr, G. F. 2004. "Proposed criteria in residential communities for low-frequency noise emissions from industrial sources." *Noise Control Engineering Journal* 52 (4):179-185.

Hessler Jr, G. F. 2005. "Proposed criteria for low frequency industrial noise in residential communities." *Low Frequency Noise, Vibration and Active Control* 24 (2):97-106.

Hetzel, R., and R. A. Putnam. 2009. "Sources and rating criteria of low frequency gas turbine exhaust noise - via case study." INTER-NOISE and NOISE-CON Congress and Conference Proceedings, 2009, Ontario, Canada, 23-26 August.

Hsu, C. M., and R. F. Huang. 2012. "Effects of crossflow on puff and oscillation modes of a pulsed elevated transverse jet." *European Journal of Mechanics-B/Fluids* 31:140-148.
Hsu, C. M., and R. F. Huang. 2014. "Comparisons of flow and mixing characteristics between unforced and excited elevated transverse jets." *Journal of Mechanics* 30:87-96.
Huang, J. F., M. J. Davidson, and R. I. Nokes. 2005. "Two-dimensional and line jets in a weak cross-flow." *Journal of Hydraulic Research* 43 (4):390-398.
Huang, R. F., and R. H. Hsieh. 2002. "An experimental study of elevated round jets deflected in a crosswind." *Experimental Thermal and Fluid Science* 27 (1):77-86.
Huang, R. F., and R. H. Hsieh. 2003. "Sectional flow structures in near wake of elevated jets in a crossflow." *American Institute of Aeronautics and Astronautics Journal* 41 (8):1490-1499.
Huang, R. F., and C. M. Hsu. 2012. "Turbulent flows of an acoustically excited elevated transverse jet." *American Institute of Aeronautics and Astronautics Journal* 50 (9):1964-1978.
Huang, R. F., and J. Lan. 2005. "Characteristic modes and evolution processes of shear-layer vortices in an elevated transverse jet." *Physics of Fluids* 17 (3):034103.
International Organization for Standardization. 1993a. ISO 9613-1:1993 Acoustics - Attenuation of sound during propagation outdoors – Part 1: Calculation of the absorption by the atmosphere.
International Organization for Standardization. 1993b. ISO 10494:1993 Gas turbines and turbine sets-Measurement of emitted airborne noise – Engineering/ survey method.
International Organization for Standardization. 1996. ISO 9613-2:1996 Acoustics - Attenuation of sound during propagation outdoors – Part 2: General method of calculation.
Johnson, B. E., G. S. Elliott, and K. T. Christensen. 2013. "Structural characteristics of a heated jet in cross-flow emanating from a raised, circular stack." *Experiments in Fluids* 54 (6):1543. doi: 10.1007/s00348-013-1543-1.
Kudernatsch, G. 2000. "Combustion turbine exhaust systems-low frequency noise reduction." INTER-NOISE 2000, The 29th International Congress and Exhibition on Noise Control Engineering, Nice, France, 27-30 August.
Leav, O. Y., B. S. Cazzolato, and C. Q. Howard. 2015. "Directivity analysis of sound in turbulent exhaust jets with laminar cross-flow: A numerical study." Acoustics 2015, Hunter Valley, Australia, 15-18 November.
Leav, O. Y., B. S. Cazzolato, and C. Q. Howard. 2017. "A computational analysis of sound directivity from sound propagation through non-isothermal, turbulent exhaust jets in cross-flow." 24th International Congress of Sound and Vibration, London, United Kingdom, 23-27 July.
Mungur, P., H. E. Plumblee, and P. E. Doak. 1974. "Analysis of acoustic radiation in a jet flow enviroment." *Journal of Sound and Vibration* 36 (1):21-52.